Highlights on Spanish Astrophysics X, Proceedings of the XIII Scientific Meeting of the Spanish Astronomical Society held on July 16 – 20, 2018, in Salamanca, Spain. B. Montesinos, A. Asensio Ramos, F. Buitrago, R. Schödel, E. Villaver, S. Pérez-Hoyos, I. Ordóñez-Etxeberria (eds.), 2019

The complexity and richness of the Galactic disc velocity field unveiled by Gaia DR2.

Romero-Gómez, M.[1], Antoja, T.[1], Figueras, F.[1], Mateu, C.[2], Aguilar, L.A.[3] Castro-Ginard, A.[1], Carrasco, J.M.[1], and Masana, E.[1]

[1] Institut de Ciències del Cosmos, Universitat de Barcelona (IEEC-UB), Martí i Franquès 1, E-08028 Barcelona, Spain
[2] Departamento de Astronomía, Instituto de Física, Universidad de la República, Iguá 4225, CP 11400 Montevideo, Uruguay
[3] Instituto de Astronomía, Universidad Nacional Autonóma de México, Apdo. Postal 877, Ensenada, 22800 Baja California, Mexico

Abstract

In this talk, we summarise the main results from the Gaia data release (GDR2) science demonstration paper on the Milky Way disc kinematics. GDR2 provides the largest existing full 6D phase-space coordinates catalogue. We benefit for the first time from a sample of 4.9 million stars with full 6-D phase-space coordinates, precise parallaxes (with a relative error less than 20%) and precise Galactic cylindrical velocities (median uncertainties of 0.9-1.4 km/s and 36% of the stars with uncertainties smaller than 1 km/s on all 3 components). The 2.4 million giant stars from this sample map the velocity field of the galactic disc from about 5 to 13 kpc from the galactic centre. We also study the distribution of 0.3 million solar neighbourhood stars (r < 200 pc), with impressive median velocity uncertainties of 0.4 km/s. The maps show the complexity and richness of the velocity field of the galactic disc

1 Introduction

Gaia Data Release 2 was published in April 2018 providing the five-parametric astrometric solution for 1.3 billion sources up to magnitude G $\sim$ 21 mag (positions, parallaxes and proper motions). For a subset of 7.2 million sources brighter than $G_{RVS} = 12$ mag and with effective temperature in the range $\sim [3550, 6900]$ K, it also provides line-of-sight velocities. This allows for the first time to study kinematic maps for a large amount of stars that extend well beyond the immediate vicinity of the Sun. The precision of the line-of-sight velocities are at the $\mathrm{km\,s^{-1}}$level being, at the bright end, of the order of 0.2 $\mathrm{km\,s^{-1}}$and, at the faint end, of the order of 1.4 $\mathrm{km\,s^{-1}}$(for $\mathrm{T}_{eff} = 5000$ K) and of the order of 3.7 $\mathrm{km\,s^{-1}}$(for $\mathrm{T}_{eff} = 6500$ K).

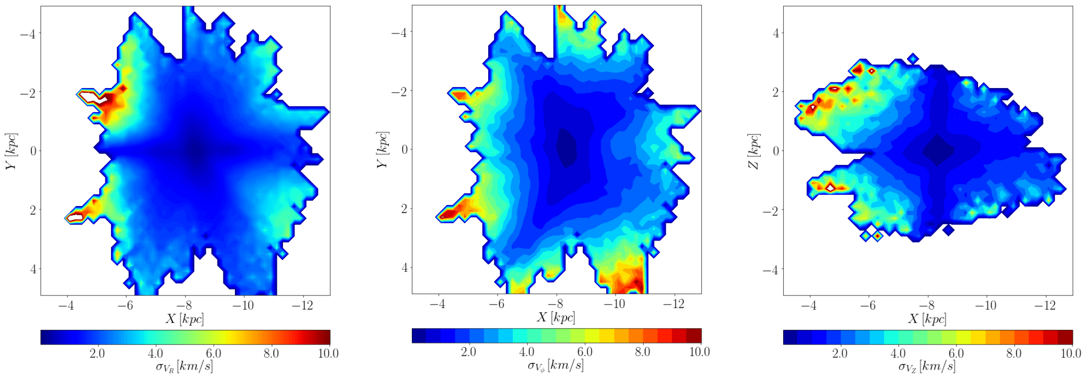

Figure 1: Median uncertainties in V_R, V_ϕ and V_Z (form left to right) for the giant sample. Note that for the uncertainties in V_R and V_ϕ, we use the (X,Y) galactocentric cartesian projection, while for the V_Z, we use the (X,Z) plane projection.

2 Mapping the Milky Way disc kinematics

Out of the 7.2 million sources with line-of-sight velocities, we select those with relative error in parallax smaller than 20 % and galactocentric cylindric distance between $5 < R < 13$ kpc, up to magnitude $G < 13$. This reduces the sample to 6.4 high quality sources, and we refer to it as the Main sample. From the Main sample, we select the giant stars by using a de-reddened HR diagram using 2MASS photometry (see [5] for details). We select the giants by requiring that the absolute magnitude in G band $M_G < 3.9$ and intrinsic colour $(G_{BP} - G_{RP})_0$ >0.95. The Giants sample contains ~ 3.1 million sources.

The kinematic maps shown below are represented in galactocentric cylindric coordinates, whose errors are obtained using the full covariance matrix and the inverse of the parallax as the distance estimator.

Figure 1 shows the median uncertainties in the radial, tangential and vertical directions for the giant sample in the (X,Y) projection (with $|Z| < 200\ pc$) for the radial and tangential components and in the (X,Z) projection (with $|Y| < 200\ pc$) for the vertical component. The median uncertainties are $(\epsilon_{V_R}, \epsilon_{V_phi}, \epsilon_{V_Z}) = (1.4, 1.4, 0.9)$ $\mathrm{km\,s^{-1}}$ and about 20% of the giant stars have all velocity components with a median uncertainty smaller than 1 $\mathrm{km\,s^{-1}}$.

The high quality of the giants sample allows to compute kinematic maps in different cuts in Z, to make 3-dimensional views of the motion of the stars in a large sphere. In the top panels of Fig. 2 we show the face-on views of the kinematics in the mid plane $[-200, 200]$ pc. To make a comparison of what we should expect from an axisymmetric distribution in equilibrium, we show the same projection for an ensemble of test particles relaxed in an axisymmetric disc [7]. Note the large streaming motion in both velocity components, some of them already known (see [5] for details) and some new features, which depart from the equilibrium and axisymmetric conditions.

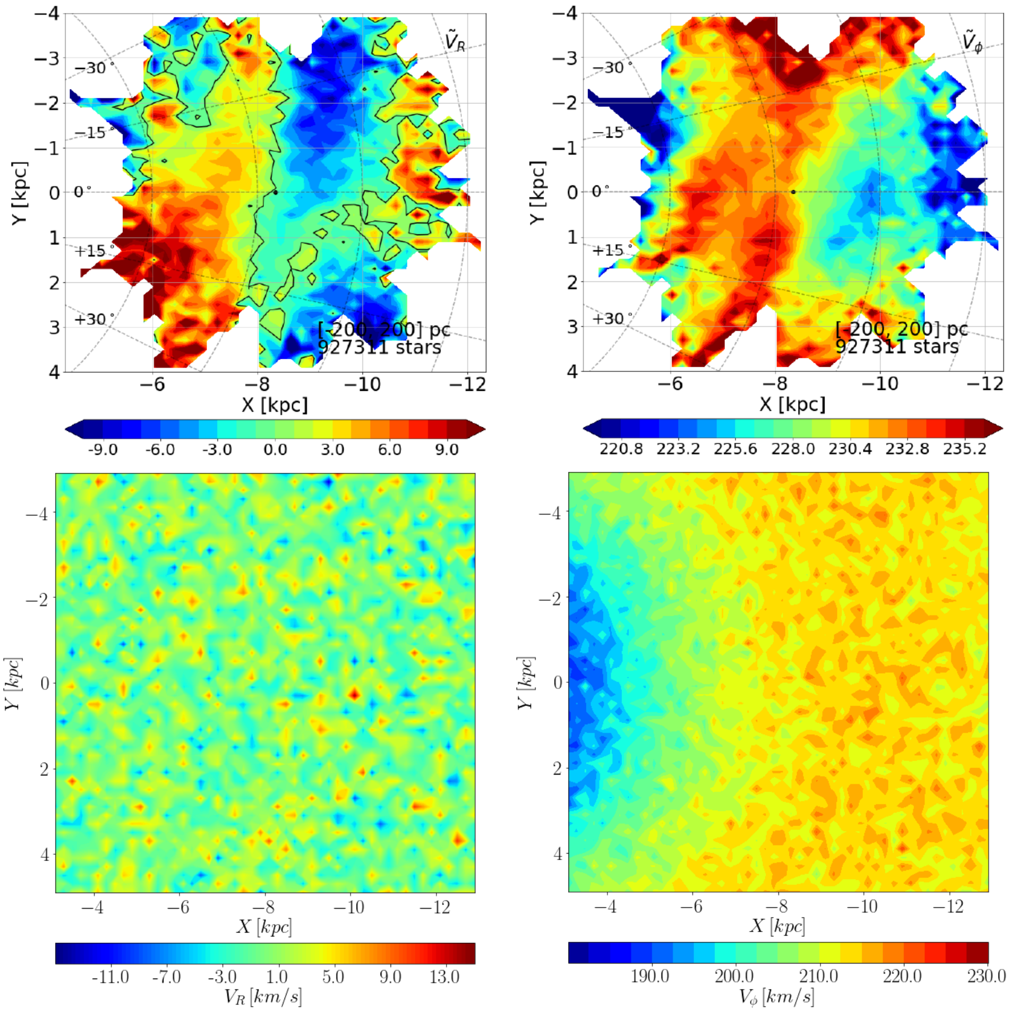

Figure 2: Face-on views of the kinematics in the mid plane $[-200, 200]$ pc, medians in radial and tangential velocities (left and right panels, respectively). Top row: for the giant sample. Bottom row: for an axisymmetric disc in equilibrium.

3 The Galactic warp signature using disc kinematics

In this section we focus on the vertical component and its applications to characterise the Galactic warp of the Milky Way. We use a different sample from that in Sect. 2. We develop the methods to study the warp in such a way they work as much as possible in the observable space, so, we only need the proper motions: μ_l^* and μ_b in the galactic longitude and latitude directions, respectively. Therefore, we select sources from the Gaia Data Release 2 with full 5-astrometric solution. From the 1.3 billion sources, we select stars with parallaxes up to magnitude G$\sim$ 20 and with absolute value of the relative error in parallax smaller than 50%. For these stars, we compute bayesian distances, d, with an exponentially decreasing space density prior with scale-length $L = 2$ kpc (see Romero-Gomez et al (2018, in preparation) for details). We then remove the cool main sequence stars by applying the cut: $M'_G < 1.95*(G_{BP} - G_{RP})+2.$, following the extinction line, where M'_G is the absolute G magnitude of the star uncorrected for extinction; M'_G is given by $M'_G = G - 5\log 10(d) + 5$; and $(G_{BP} - G_{RP})$ is the observed colour. We compute the absorption in V using Drimmel extinction model [3], and a fit to obtain the absorption in the G band and the colour excess (Carrasco, private communication). From the de-reddened HR diagram, we select two intrinsically bright populations with different ages: an OB-type sample if young stars: $M_G < 2.$ and $(G_{BP} - G_{RP})_0 < 0$; an the Red Giant Branch (RGB): $M_G < 3.9$ and $(G_{BP} - G_{RP})_0 > 0.95$.

The two methods developed in the research group are the LonKin method and the nGC3 PCM method. The former relies on selecting stars in cylindrical radial rings and plotting the median proper motion in latitude, with respect to the Local Standard of Rest, as a funcion of the galactic longitude. If the Galactic disc is flat, the median $\mu_{b,LSR}$ should be constant and equal to zero, but if it is warped, a particular variation will be introduced as a function of l. If the disc is symmetrically warped and the line-of-nodes is aligned with the Sun-Galactic Centre line, the LonKin method predicts a maximum in $\mu_{b,LSR}$ in the anticentre direction. The nGC3 method of the family of Great Circle Cell Counts (hereafter, GC3) methods [4, 6] searches for overdensities in great circle cells in the sky, by sweeping over the sky counting how many stars have position and velocities (nGC3 does not require line-of-sight velocities) lying in a great circle within a given tolerance, each great circle being defined uniquely by its normal vector or *pole*. The all-sky sweep over all possible great circle cells results in a Pole Count Map (hereafter, PCM). If the Galactic disc were flat, the peak in stellar density would be located in the North Galactic Pole of the PCM. If the disc is not flat, the peak of over-density moves in the PCM providing information on the amplitude and tilt angle of the warp, as well as the azimuth (twist) of the line-of-nodes as a function of radii (see [1] for detailed examples).

In Fig. 3, we show the result of applying the LonKin method to the OB (left) and RGB samples (right). We use a different color for each radial ring. Note that, the larger the radius, the larger the value of $\mu_{b,LSR}$, as expected. Note as well, that the trend is not smooth and that the $\mu_{b,LSR}$ does not peak in the anticentre direction, indicating that the Galactic warp is not symmetric. We also note a clear difference between the two populations. The amplitude of the warp is larger in the RGB sample, than in the OB, and we also detect that the warp onset radius is slightly larger for the OB than for the RGB, in agreement with

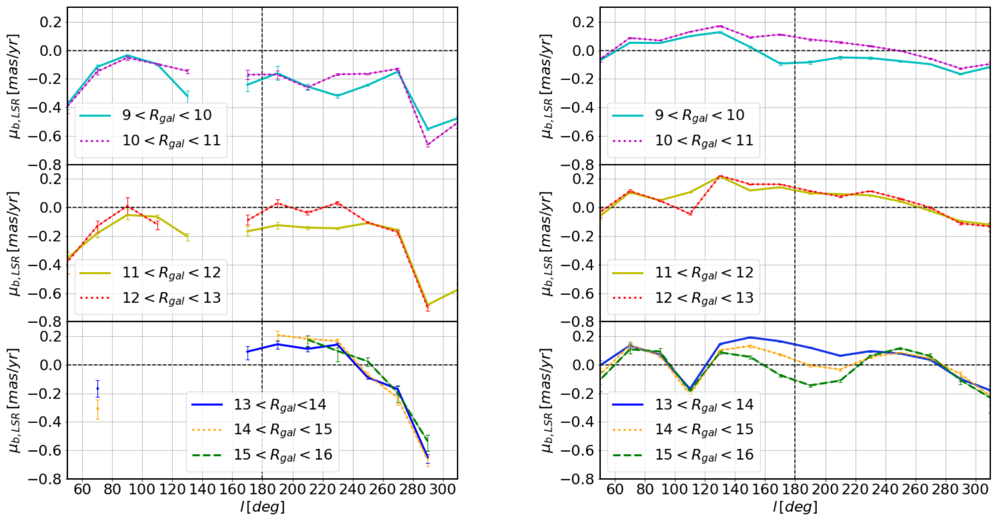

Figure 3: LonKin method applied to the OB and RGB samples (left and right panels, respectively). From top to bottom, different radial cylindrical galactocentric rings specified in the legend. Only bins in longitude with at least 300 stars are plotted. Horizontal dashed line shows the zero-axis while the vertical dashed line shows the anticenter direction at 180 deg, the error bars show the lower and upper 1σ uncertainty.

previous studies that estimate that the starting radius of the warp is anti-correlated with the age of the population [2].

In Fig. 4, we show the results of applying the nGC3 method to both samples (OB, top and RGB, bottom). We show the PCM per radial shell in each column, moving outwards from left to right. We observe how as a function of radius, a secondary peak appears detached from the one in the North Galactic Pole (corresponding to stars in the flat disc), indicating that, again, the Galactic warp is not symmetric. We also see that the secondary peak appears at a different radial bin depending on the population: in the panel $R \in [13, 14]$ kpc in the OB sample, while it is clear at the bin $R \in [12, 13]$ kpc in the RGB sample, in agreement with the LonKin method. The position of the secondary peak indicates a clear Lopsided warp.

4 Conclusions

So, in this talk, we show that Gaia Data Release 2 reveals a rich and complex kinematic structure in the disc. The sample with line-of-sight velocities points to the fact that the disc is not in equilibrium, and models need to be adapted to fit the complexity of the data. The study of the vertical velocities, without the need of line-of-sight velocities, to tackle the Galactic warp, reveal, again, the fact that the disc is not in equilibrium, that the data do reflex the expected motion of a warped disc, but this is not symmetric at both sides.

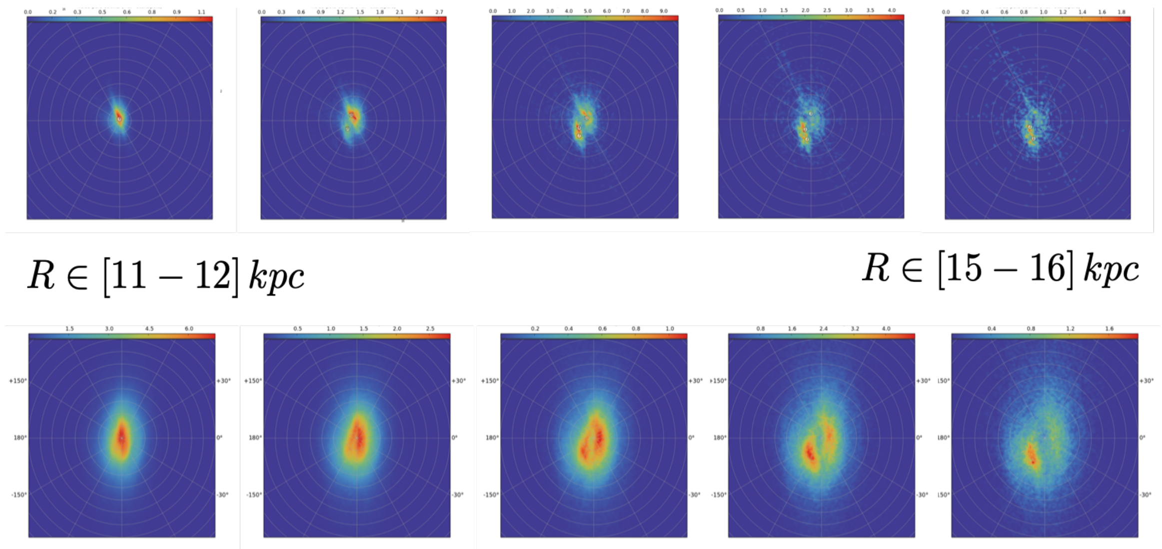

Figure 4: nGC3 PCM applied to OB and RGB samples (top and bottom rows, respectively), the radial shells increasing from left to right.

Acknowledgments

This work was supported by the MINECO (Spanish Ministry of Economy) - FEDER through grant ESP2014-55996-C2-1-R and MDM-2014-0369 of ICCUB (Unidad de Excelencia "María de Maeztu"), the European Community's Seventh Framework Programme (FP7/2007-2013) under grant agreement GENIUS FP7 - 606740. We also acknowledge the team of engineers (GaiaUB-ICCUB) in charge to set up and maintain the Big Data platform (GDAF) at University of Barcelona. CM is grateful for the hospitality and support from ICCUB and IA-UNAM, where part of this research was carried out. We thank the PAPIIT program of DGAPA/UNAM for their support through grant IG100319.

References

[1] Abedi, H. and Mateu, C. and Aguilar, L. A. and Figueras, F. and Romero-Gómez, M. 2014, MNRAS, 442, 3627

[2] Amôres, E. B. and Robin, A. C. and Reylé, C. 2017, A&A, 602, 67

[3] Drimmel, R.; Cabrera-Lavers, A.; López-Corredoira, M. 2003, A&A, 409, 205

[4] Johnston, K. V. and Hernquist, L. and Bolte, M. 1996, ApJ, 465, 278

[5] Katz, D., Antoja, T., Romero-Gomez, M. et al (Gaia Collaboration) 2018, A&A, 616, 11

[6] Mateu, C. and Bruzual, G. and Aguilar, L. and Brown, A. G. A. and Valenzuela, O. and Carigi, L. and Velázquez, H. and Hernández, F. 2011, MNRAS, 415, 214

[7] Romero-Gómez, M., Figueras, F., Antoja, T., Abedi, H., Aguilar, L. 2015, MNRAS, 447, 218